International Journal of
Molecular Sciences

MDPI

Article

Zebrafish Mutant Lines Reveal the Interplay between *nr3c1* and *nr3c2* in the GC-Dependent Regulation of Gene Transcription

Alberto Dinarello [1], Annachiara Tesoriere [1], Paolo Martini [2], Camilla Maria Fontana [1], Davide Volpato [1], Lorenzo Badenetti [1], Francesca Terrin [1], Nicola Facchinello [1], Chiara Romualdi [1], Oliana Carnevali [3], Luisa Dalla Valle [1,*,†] and Francesco Argenton [1,†]

[1] Department of Biology, University of Padova, 35121 Padova, Italy; alberto.dinarello@phd.unipd.it (A.D.); annachiara.tesoriere@phd.unipd.it (A.T.); camillamaria.fontana@phd.unipd.it (C.M.F.); davide.volpato.4@studenti.unipd.it (D.V.); lorenzo.badenetti@phd.unipd.it (L.B.); francesca.terrin@phd.unipd.it (F.T.); nicola.facchinello@unipd.it (N.F.); chiara.romualdi@unipd.it (C.R.); francesco.argenton@unipd.it (F.A.)
[2] Department of Molecular and Translational Medicine, University of Brescia, 25121 Brescia, Italy; paolo.martini@unibs.it
[3] Department of Life and Environmental Sciences, Università Politecnica delle Marche, 60131 Ancona, Italy; o.carnevali@univpm.it
* Correspondence: luisa.dallavalle@unipd.it
† These authors contributed equally to this work.

Abstract: Glucocorticoids mainly exert their biological functions through their cognate receptor, encoded by the *nr3c1* gene. Here, we analysed the glucocorticoids mechanism of action taking advantage of the availability of different zebrafish mutant lines for their receptor. The differences in gene expression patterns between the zebrafish *gr* knock-out and the gr^{s357} mutant line, in which a point mutation prevents binding of the receptor to the hormone-responsive elements, reveal an intricate network of GC-dependent transcription. Particularly, we show that Stat3 transcriptional activity mainly relies on glucocorticoid receptor GR tethering activity: several Stat3 target genes are induced upon glucocorticoid GC exposure both in wild type and in $gr^{s357/s357}$ larvae, but not in *gr* knock-out zebrafish. To understand the interplay between GC, their receptor, and the mineralocorticoid receptor, which is evolutionarily and structurally related to the GR, we generated an *mr* knock-out line and observed that several GC-target genes also need a functional mineralocorticoid receptor MR to be correctly transcribed. All in all, zebrafish mutants and transgenic models allow in vivo analysis of GR transcriptional activities and interactions with other transcription factors such as MR and Stat3 in an in-depth and rapid way.

Keywords: glucocorticoid receptor; mineralocorticoid receptor; zebrafish; CRISPR/Cas9

check for updates

Citation: Dinarello, A.; Tesoriere, A.; Martini, P.; Fontana, C.M.; Volpato, D.; Badenetti, L.; Terrin, F.; Facchinello, N.; Romualdi, C.; Carnevali, O.; et al. Zebrafish Mutant Lines Reveal the Interplay between *nr3c1* and *nr3c2* in the GC-Dependent Regulation of Gene Transcription. *Int. J. Mol. Sci.* **2022**, *23*, 2678. https://doi.org/10.3390/ijms23052678

Academic Editors: George P. Chrousos and Nicolas C. Nicolaides

Received: 27 January 2022
Accepted: 24 February 2022
Published: 28 February 2022

Publisher's Note: MDPI stays neutral with regard to jurisdictional claims in published maps and institutional affiliations.

Copyright: © 2022 by the authors. Licensee MDPI, Basel, Switzerland. This article is an open access article distributed under the terms and conditions of the Creative Commons Attribution (CC BY) license (https://creativecommons.org/licenses/by/4.0/).

1. Introduction

The glucocorticoid receptor (GR) is encoded by the *NR3C1* gene and normally localized in the cytoplasm in a multimeric complex composed of heat shock protein (HSP) 70 and 90 and immunophilins. When glucocorticoids (GCs) bind to GR, the FK506-binding protein 51 (FKBP51) is substituted by FKBP52 and dynein is recruited to allow the migration of GC/GR in the nucleus [1]. Once in the nucleus, GR detaches from HSP90 [2] and regulates the transcription of target genes directly interacting with DNA at the level of hormone response elements (HRE). HREs are cis elements shared with other steroid receptors such as the mineralocorticoid receptor (MR), the androgen receptor (AR) or the progesterone receptor (PR) [3]. Additionally, GR can affect the activity of other transcription factors through tethering or complex protein–protein–DNA interactions described in Ratman et al. [4]. The lack of GR in mice is lethal: *Nr3c1* knock-out (KO) animals die after birth for severe delay of lung development [5]. On the other hand, $Gr^{dim/dim}$ mice, characterized by the A458T

mutation in the second zinc finger that abrogates GR dimerization and the subsequent HRE-dependent transactivation, are vital and reach adulthood, hence underlining alternative GR-dependent mechanisms of transcription activation [6]. Although GR monomers expressed by $Gr^{dim/dim}$ mice mutants have been proven to bind DNA efficiently [7,8], recent data obtained by Johnson and collaborators demonstrated that GR monomers poorly bind to chromatine and induce the transcription of a restricted number of GC-related genes [9].

However, with reduced transcriptional activity, GR monomers can indeed bind several transcription factors such as nuclear factor κ-light-chain-enhancer of activated B cells (NF-κB), signal transducer and activator of transcription 3 (STAT3) and activator protein-1 (AP-1) [10,11] and thus the $Gr^{dim/dim}$ model can allow discriminating between GR activity as dimer or monomer.

As recently reviewed by Dinarello et al. [12], in the last 20 years, zebrafish has gained importance for the study of GC/GR activities and several mutants have been generated for the genes encoding GR or the enzymes involved in the synthesis of GCs. In zebrafish, GR is encoded by a single gene called *nr3c1*, which shares a high similarity with the human orthologue [13].

In this work, taking advantage of two zebrafish mutant lines, the $nr3c1^{ia30}$ [14] and the $nr3c1^{s357}$ [15,16], we decided to better investigate in vivo the different mechanisms used by GR in the regulation of gene transcription. The $nr3c1^{ia30}$ (herein called $gr^{ia30/ia30}$) line has been generated with CRISPR/Cas9 technology and is characterized by an insertion of 5 nucleotides in the second exon of the *nr3c1* gene. This mutation leads to a frameshift and a premature stop codon, and the mutation affects the response to stress stimuli, the feeding entrainment of zebrafish circadian clock and reproduction [14,17,18]. On the other hand, the $nr3c1^{s357}$ mutant line, generated with N-ethyl-N-nitrosourea (ENU) mutagenesis, has a point mutation that prevents GR interaction with the DNA [19]. However, $nr3c1^{s357/s357}$ mutants (herein called $gr^{s357/s357}$) can still synthesize an entire GR protein (replacing an arginine 443 with a cysteine in the second zinc finger) available for interaction with other possible proteins and, hence, retaining all its HRE independent transcriptional activities. Starting from the experimental evidence shown by Facchinello et al. [14] and Vettori et al. [20], we wanted to analyse in more detail the differences between these two *gr* mutant lines, aiming to show how their use can help to uncover the functions that GR accomplishes by directly interacting with the DNA and the processes affected through the regulation of other transcription factors.

A complete evaluation of GR activity as a transcription factor cannot disregard the role of MR, that, interacting with GR in heterodimeric or heterotetrametic complexes, seems to regulate GR-dependent activities [21,22], affecting the response to GCs at the transcriptional level. In detail, GR and MR can interact with each other [23,24] and the heterodimer can affect gene transcription, thus increasing the potential roles of GC in tissues such as the brain, that expresses both receptors [22,24,25]. Consequently, the MR:GR ratio is critical for the maintenance of neuronal functions [26] and its imbalance was connected to behavioural dysfunctions, cognitive disorders [27] and depression in humans [28–30]. The higher expression of MR in the teleost brain also suggests that, in zebrafish, MR has a major role in regulating stress axis behaviour [31,32].

The GR and MR collaboration in the regulation of target genes transcription is particularly interesting in teleosts. GR and MR are structurally, evolutionarily, and functionally tightly connected [33] but, while in mammals MR also binds a specific ligand, aldosterone, and regulates ion balance and homeostasis [21,34], it has been demonstrated that in zebrafish GR accomplishes these functions [35–40]. Hence, in zebrafish, MR exerts only cortisol-related activities and *Danio rerio* can be an excellent model to study all the MR/cortisol-dependent processes that are also conserved in mammals, such as obesity, heart failure and depression [21]. For these reasons and to better elucidate the interplay between GR and MR, we decided to generate a new *mr* (*nr3c2*) KO zebrafish line with CRISPR/Cas9 technology, to investigate the role of MR in the regulation of GC/GR-dependent transcription.

2. Results

2.1. The Expression of GC-Dependent Genes klf9, epas1a and ucp2 Confirms Differences between $gr^{ia30/ia30}$ and $gr^{s357/s357}$ Mutants' GCs Response

Prior to the analysis of the differences between the two *gr* mutant lines at the transcriptional level, we confirmed the downregulation of *nr3c1* mRNA expression only in $gr^{ia30/ia30}$ compared to $gr^{+/+}$ siblings (named $gr^{+/+1}$, to distinguish them from $gr^{+/+2}$, siblings of $gr^{s357/s357}$ larvae) (Figure 1A,B). Therefore, only in the $gr^{ia30/ia30}$ mutants the protein is absent or, when present, it is truncated and completely non-functional.

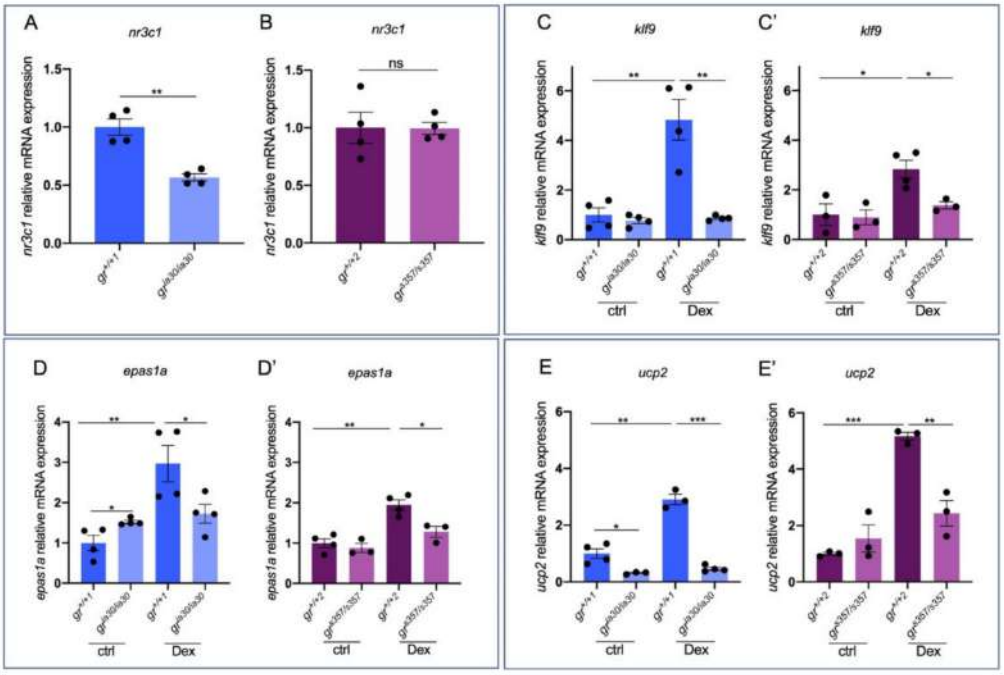

Figure 1. GR direct target genes show slight differences of expression between gr^{ia30} and gr^{s357} mutant lines. (**A**) RT-qPCR analysis of *nr3c1* in 6 dpf $gr^{+/+1}$ and $gr^{ia30/ia30}$ larvae. (**B**) RT-qPCR analysis of *nr3c1* in 6 dpf $gr^{+/+2}$ and $gr^{s357/s357}$ larvae. (**C**) RT-qPCR analysis of *klf9* in 6 dpf $gr^{+/+1}$ and $gr^{ia30/ia30}$ (**C**) and in $gr^{+/+2}$ and $gr^{s357/s357}$ (**C'**) larvae with or without Dex treatment. (**D**) RT-qPCR analysis of *epas1a* in 6 dpf $gr^{+/+1}$ and $gr^{ia30/ia30}$ (**D**) and in $gr^{+/+2}$ and $gr^{s357/s357}$ (**D'**) larvae with or without Dex treatment. (**E**) RT-qPCR analysis of *ucp2* in 6 dpf $gr^{+/+1}$ and $gr^{ia30/ia30}$ (**E**) and in $gr^{+/+2}$ and $gr^{s357/s357}$ (**E'**) larvae with or without Dex treatment. Statistical analyses were performed with Student's *t* test. Mean ± SEM. * $p < 0.05$; ** $p < 0.01$; *** $p < 0.001$.

Mainly, our experimental approach was based on RT-qPCR analysis of the expression of GC-dependent genes in basal conditions or after 6 h of treatment with the synthetic GC Dexamethasone (Dex).

Since both lines, $gr^{ia30/ia30}$ and $gr^{s357/s357}$, lack a GR that can bind to HREs (respectively due to *gr* KO and to the point mutation in GR DNA-binding domain), we found the expression of GR direct target genes significantly dampened in both lines. As already reported by Facchinello and collaborators [14], two important GC/GR target genes like *fk506-binding protein 5* (*fkbp5*), which belongs to the negative feedback loop induced by GC/GR for self-regulation, and *forkhead box protein O 3b* (*foxo3b*), which is upregulated by GCs [41], are significantly downregulated in both mutant lines compared to wild type (WT) and, in both $gr^{ia30/ia30}$ and $gr^{s357/s357}$ homozygous mutants, Dex treatment does not induce the expression of these two genes.

Here, as reported in Figure 1C,D, we confirmed the previous results by analysing the expression of other two GC/GR-dependent genes: *krueppel-like factor 9* (*klf9*), whose GC-dependent induction has a pro-inflammatory effect upon prolonged cortisol exposure [42], and *endothelial PAS domain protein 1a* (*epas1a*), a GC-regulated gene that encodes for hypoxia-

inducible factor 2α (HIF2α) [43,44]. These results demonstrate that both mutant lines cannot induce the expression of *klf9* and *epas1a* when exposed to exogenous GCs, confirming that HRE-related gene transcription cannot be properly induced in both mutant lines. Of note, in $gr^{ia30/ia30}$ line, at the basal level the *epas1a* expression is significantly upregulated, suggesting that the high levels of cortisol in $gr^{ia30/ia30}$ larvae [14] can determine the upregulation of GC-target genes probably acting via other steroid hormone receptors, such as the MR that has a high affinity for cortisol [26].

Furthermore, we measured the level of expression of *uncoupling protein 2* (*ucp2*) that encodes for a proton transporter [45] and allows the GCs regulation of mitochondrial biogenesis in muscle [46]. Interestingly, it is severely downregulated in $gr^{ia30/ia30}$ compared to $gr^{+/+1}$. On the other hand, no significant differences were observed between $gr^{+/+2}$ and $gr^{s357/s357}$, thus revealing a basal differential expression of *ucp2* in $gr^{ia30/ia30}$ and $gr^{s357/s357}$. While a 6 h long treatment with Dex in $gr^{+/+1}$ determines an upregulation of this gene, both mutant lines appeared to be insensitive to Dex treatment since we could not detect significant differences in *ucp2* expression levels between treated and untreated mutants, suggesting that this gene is properly activated via the DNA-binding domain (Figure 1E).

These results confirmed that direct DNA-binding-dependent GC-induced transcription is significantly dampened in these two lines, even if some small differences are evident.

2.2. Analysis of GC-Dependent Transcription in mr Mutant Zebrafish Larvae

As mentioned above, MR is an important modulator of GR activity for its capability to regulate GC-dependent transcription generating MR/GR heterodimers and heterotetramers and to bind HRE promoter regions on DNA. MR is encoded by the *nr3c2* gene and in zebrafish has a high affinity for cortisol and for 11-deoxycorticosterone (DOC) [31]. To test whether MR has a function in the different expression patterns of gr^{ia30} and gr^{s357} zebrafish lines and to evaluate the possible roles of MR/GR interaction in the expression of GC-target genes, we decided to generate a new *nr3c2* zebrafish mutant line with CRISPR/Cas9 approach. The $nr3c2^{ia32/ia32}$ (herein called $mr^{ia32/ia32}$) zebrafish mutant line is characterized by a deletion of 11 nucleotides in the third exon of the *nr3c2* gene. This mutation determines a frameshift with the subsequent generation of a premature stop codon (Figure S1A–D). Homozygous mutants are predicted to encode an aberrant, truncated protein of 628 amino acids, 17 of which are determined by the mutation. The mutated MR lacks the DBD, the LBD and the activation domain in the C-terminus (Figure S1A).

Moreover, homozygous mutants are also characterized by a significant reduction of *nr3c2* mRNA expression compared with $mr^{+/+}$ siblings (Figure 2A), possibly due to the nonsense-mediated mRNA decay (NMD) commonly activated in KO zebrafish lines [47]. $mr^{+/+}$, $mr^{+/ia32}$ and $mr^{ia32/ia32}$ animals can be easily distinguished by PCR with the primers listed in Table 1 (Figure S1E). Homozygous mutants are viable and reach adulthood, even if the mutation has some effects on survival: as reported in Figure S1F, the percentage of mutants observed at one-month post-fertilization is significantly lower (17%) than the expected one (25%). Interestingly, *nr3c1* mRNA expression is more upregulated in $mr^{ia32/ia32}$ larvae than $mr^{+/+}$ siblings (Figure 2B), suggesting that compensation mechanisms are triggered in this mutant line. Of note, *nr3c2* mRNA levels are significantly higher in *gr* homozygous mutants compared to WT siblings, while this transcript is significantly downregulated in $gr^{s357/s357}$ mutants compared to WT (Figure 2C,D), showing another substantial difference between these two *gr* mutant lines.

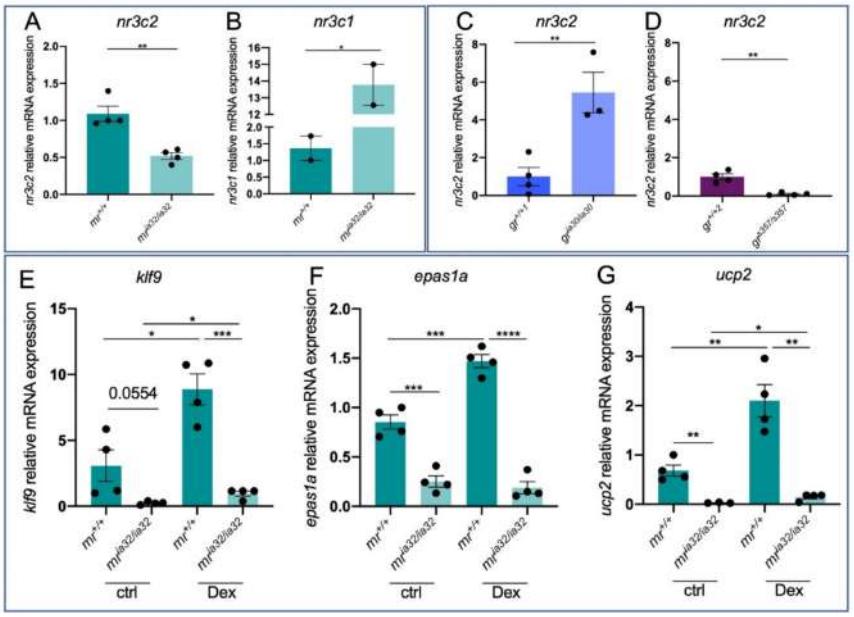

Figure 2. Analysis of GC-dependent genes in *mr* mutant zebrafish larvae. (**A**) RT-qPCR analysis of *nr3c2* in 6 dpf $mr^{+/+}$ and $mr^{ia32/ia32}$. (**B**) RT-qPCR analysis of *nr3c1* in 6 dpf $mr^{+/+}$ and $mr^{ia32/ia32}$. (**C**) RT-qPCR analysis of *nr3c2* in 6 dpf $gr^{+/+}$ and $gr^{ia30/ia30}$. (**D**) RT-qPCR analysis of *nr3c2* in 6 dpf $gr^{+/+}$ and $gr^{s357/s357}$. (**E**) RT-qPCR analysis of *klf9* in 6 dpf $mr^{+/+}$ and $mr^{ia32/iaq32}$ larvae with or without Dex treatment. (**F**) RT-qPCR analysis of *epas1a* in 6 dpf $mr^{+/+}$ and $mr^{ia32/ia32}$ larvae with or without Dex treatment. (**G**) RT-qPCR analysis of *ucp2* in 6 dpf $mr^{+/+}$ and $mr^{ia32/ia32}$ larvae with or without Dex treatment. Statistical analyses were performed with Student's *t* test. Mean ± SEM. * $p < 0.05$; ** $p < 0.01$; *** $p < 0.001$; **** $p < 0.0001$.

Table 1. List of primers (5′–3′ sequences) used for genotyping and for RT-qPCR.

Gene	Forward Sequence (5′–3′)	Reverse Sequence (5′–3′)	Use
nr3c1	ACCACTTCAAGCGGACAGAG	CCGGCTTCTGATCTTTCTGC	Genotyping
nr3c2	GACAGCCAAAGTGTGTCTGG	TGAGTCTTACCTTCTACCGCTC	Genotyping
stat3	GGCCTCTCTGATAGTGACCG	GCATTGTATAAAGCGCTACAGAG	Genotyping
ube2a	CATCATGGTCTGGAACGCTG	GAGGAAACGTCATATGTTGGAC	RT-qPCR
nr3c1	CAACACAATTACCTGTGTGCTG	CTTGACGTGCCTTTGACTTGC	RT-qPCR
nr3c2	CTGAGGCACACGTCTTCG	CAGCACAAAGGTAGTTGTGC	RT-qPCR
klf9	GACCGACTGCACGCATCC	TTTTGCACAGCCAGGCCAG	RT-qPCR
epas1a	CCTACGACATGGGCGAAATA	GTCGCCTCTTCAAACTCTGC	RT-qPCR
ucp2	CACTGGACACCGCAAAAGTT	CGTACCAAAGACCCCTCGAT	RT-qPCR
slc25a25a	CTGCCGAAAACATTCCCAA	CCTCCACCACATCCCAGTTA	RT-qPCR
ucp3	GTGATGAGGGGTGTTCGAGG	TAGGTTATCTGTCATGAGGTCG	RT-qPCR
socs3a	GGAAGACAAGAGCCGAGACT	GCGATACACACCAAACCCTG	RT-qPCR
ulk2	GAAAGCAGCTCAGCTTCTGG	TCTGTGAGGCGACGGCAC	RT-qPCR
hif1al	ATGGGTGAGGTATGGGTTCG	AGAGCACACTTACCCACACA	RT-qPCR
pnpla3	CCTCTGGACGACTCTGTGTT	CGGAAGGCAGGAGGGATTAA	RT-qPCR
ddit4	GACTCTGACTCCGACAACC	TTACACAACGCCTCTTCAGTG	RT-qPCR
pomca	TGTCGAGACCTCAGCACAG	TGCGAGGAGGTCGATTTGC	RT-qPCR
fkbp5	GTGTTCGTCCACTACACC	TCTCCTCACGATCCCACC	RT-qPCR

The upregulation of *nr3c1* transcript and the possible compensatory effect that characterizes $mr^{ia32/ia32}$ mutants is further supported by the higher fluorescence intensity of $mr^{ia32/ia32}$ and $mr^{+/ia32}$ larvae in $Tg(9xGCRE\text{-}Hsv.Ul23:EGFP)^{ia20}$ background (the zebrafish reporter line of GC-related transcription described by Benato et al. [48]) when compared to $mr^{+/+}$ siblings (Figure S2A). This phenomenon probably derives from the increased expression of *nr3c1* mRNA in mutants compared to WT since, as reported by Faught and Vijayan [32] with their mr^{ca402} zebrafish KO line, the lack of Mr does not lead to hypercortisolemia, a feature that is further confirmed in the mr^{ia32} line, where the levels of expression of *pomca* are not affected in *mr* mutants compared to wild type siblings (Figure S2B).

Then, we tested the expression levels of the genes previously analysed in *gr* mutants, comparing $mr^{+/+}$ and $mr^{ia32/ia32}$ larvae and testing their responsiveness to Dex. Interestingly, *mr* KO determines a strong insensitivity to exogenous GCs since the expression levels of *klf9*, *epas1a* and *ucp2* are significantly different in treated $mr^{ia32/ia32}$ compared to treated $mr^{+/+}$ (Figure 2E–G). Additionally, it is worth noting that the lack of a functional MR significantly affects the basal expression of *epas1a* and *ucp2*. These results suggest that MR is essential for the correct GC-dependent transcriptional response and that it exerts many functions in the regulation of hypoxia response and mitochondrial homeostasis.

To better investigate this last aspect, we tested the expression of other mitochondrial proteins in the mutant lines of interest. We analysed the level of expression of *ucp3* and *solute carrier family 25 member 25* (*slc25a25*). As shown in Figure 3, these transcripts are upregulated by Dex in $gr^{+/+}$ and $mr^{+/+}$ larvae. However, while $gr^{ia30/ia30}$ show a basal lower level of expression of these transcripts compared to $gr^{+/+1}$ siblings and appear to be totally insensitive to exogenous GCs (Figure 3A,C), $gr^{s357/s357}$ larvae do not show significant differences compared to $gr^{+/+2}$ and Dex upregulates the expression of these genes either in $gr^{+/+2}$ and in $gr^{s357/s357}$ (Figure 3A′,C′). It is worth mentioning that all these transcripts are significantly downregulated in $gr^{ia30/ia30}$ compared to $gr^{+/+1}$ in basal conditions and we could not see any statistically significant difference between $gr^{+/+2}$ and $gr^{s357/s357}$, suggesting that the two mutant lines have different transcriptional profiles in basal conditions. Considering also the expression profiles of the same genes in the $mr^{ia32/ia32}$ larvae, only *ucp3* showed a reduction in basal expression in $mr^{ia32/ia32}$ larvae if compared to $mr^{+/+}$ siblings (Figure 3B,D). Interestingly, these genes do not show a response to Dex stimulation in $mr^{ia32/ia32}$, as observed in $gr^{ia30/ia30}$ (Figure 3B,D). These results suggest that possibly GR regulates the expression of these genes in a DNA-binding independent way and the expression of the identified mitochondrial proteins is also connected to MR function.

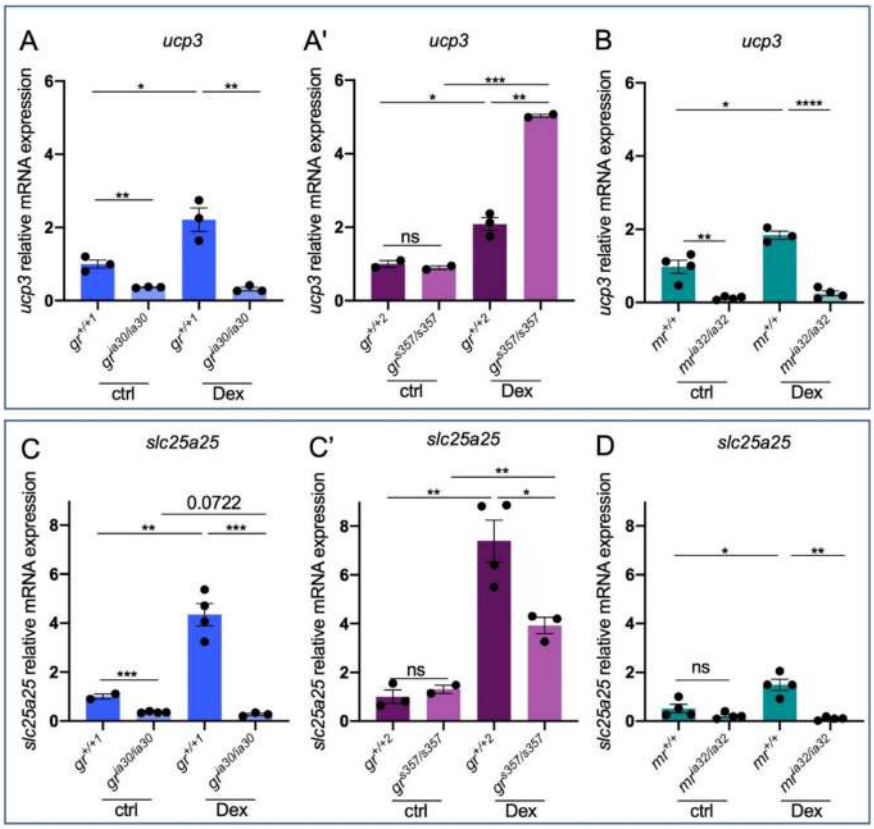

Figure 3. GC-dependent genes reveal different expression levels in the two *nr3c1* zebrafish mutant lines. (**A**) RT-qPCR analysis of *ucp3* in 6 dpf $gr^{+/+1}$ and $gr^{ia30/ia30}$ (**A**) and in $gr^{+/+2}$ and $gr^{s357/s357}$ (**A′**)

larvae with or without Dex treatment. (**B**) RT-qPCR analysis of *ucp3* in 6 dpf $mr^{+/+}$ and $mr^{ia32/ia32}$ larvae with or without Dex treatment. (**C**) RT-qPCR analysis of *slc25a25* in 6 dpf $gr^{+/+1}$ and $gr^{ia30/ia30}$ (**C**) and in $gr^{+/+2}$ and $gr^{s357/s357}$ (**C′**) larvae with or without Dex treatment. (**D**) RT-qPCR analysis of *slc25a25* in 6 dpf $mr^{+/+}$ and $mr^{ia32/ia32}$ larvae with or without Dex treatment. Statistical analyses were performed with Student's *t* test. Mean ± SEM. * $p < 0.05$; ** $p < 0.01$; *** $p < 0.001$; **** $p < 0.0001$; ns = not significant.

2.3. $gr^{ia30/ia30}$ and $gr^{s357/s357}$ Zebrafish Lines Reveal DNA-Binding Independent Mechanisms of Regulation of Stat3

The tight connection between GR and other transcription factors has already been studied [49]. Specifically, the crosstalk of GR with STAT3 was widely described by Langlais and collaborators [50]. Here, for the first time with in vivo models, we decided to better elucidate how the GR–Stat3 crosstalk works and identify some Stat3-dependent transcripts which need GR to be properly activated. The analysis of the crosstalk between GR and Stat3 allowed us to highlight again the differences between $gr^{ia30/ia30}$ and $gr^{s357/s357}$ zebrafish mutant lines. Firstly, taking advantage of the *Tg(7xStat3-Hsv.Ul23:EGFP)*^{ia28} zebrafish reporter line that expresses EGFP in Stat3-positive cells [51], we tested whether Stat3-dependent transcription in intestinal stem cells is altered in $gr^{ia30/ia30}$ and $gr^{s357/s357}$ mutant lines. Interestingly, as reported in Figure 4A, $gr^{ia30/ia30}$*;Tg(7xStat3-Hsv.Ul23:EGFP)*^{ia28} 6 dpf larvae are characterized by a significantly lower intestinal fluorescence compared to $gr^{+/+1}$*;Tg(7xStat3-Hsv.Ul23:EGFP)*^{ia28} siblings. On the other hand, we could detect a slight but not significant difference in EGFP fluorescence between $gr^{s357/s357}$*;Tg(7xStat3-Hsv.Ul23:EGFP)*^{ia28} compared to $gr^{+/+2}$*;Tg(7xStat3-Hsv.Ul23:EGFP)*^{ia28} larvae (Figure 4B). This result suggests that Stat3 transcriptional activation is different in the two *gr* zebrafish mutant lines analysed and that GR-dependent regulation of Stat3 activity relies mainly on DNA-binding independent mechanisms of GR. Interestingly, 24 h long treatment with 10 µM Dex did not affect the fluorescence of Stat3 reporter in the intestine of WT larvae (Figure S3A). Furthermore, we also decided to see whether Stat3 signalling affects GR transcriptional activity. To do so, we analysed the levels of fluorescence of the GC zebrafish reporter line *Tg(9xGCRE-Hsv.Ul23:EGFP)*^{ia20} [48] after chemical inhibition of the Stat3 pathway with AG490 (Figure 4C). No significant differences in reporter fluorescence were detected, meaning that the inhibition of Stat3 does not affect GC/GR-dependent transcription. To confirm this result, we also measured the fluorescence of *Tg(9xGCRE-Hsv.Ul23:EGFP)*^{ia20} in *stat3* mutant background, taking advantage of a $stat3^{ia23}$ zebrafish mutant line [51,52]. No significant differences between $stat3^{+/+}$, $stat3^{+/ia23}$ and $stat3^{ia23/ia23}$ 6 dpf larvae were observed (Figure S3B). Additionally, Dex treatment determines a significant increase of fluorescence in all the three genotypes analysed compared to untreated controls (Figure S3B). These results demonstrated that the lack of Stat3 does not significantly interfere with the nuclear activities of the GC/GR pathway. Moreover, a further confirmation of this result came from RT-qPCR analysis of *fkbp5* performed on $stat3^{+/+}$, $stat3^{+/ia23}$ and $stat3^{ia23/ia23}$ after Dex treatment: we could not detect significant differences in *fkbp5* expression between $stat3^{+/+}$, $stat3^{+/ia23}$ and $stat3^{ia23/ia23}$ and Dex treatment significantly induced the expression of this gene in all the genotypes under investigation (Figure S3C). However, it is worth noting that 3-day long treatment of *Tg(9xGCRE-Hsv.Ul23:EGFP)*^{ia20} with leukaemia inhibitory factor (LIF), an activator of the Jak/Stat3 pathway that upregulates the intestinal fluorescence of Stat3 reporter line (Figure S3D), determines a significant upregulation of GC reporter fluorescence (Figure 4C,C′), demonstrating that the overstimulation of the Jak/Stat3 pathway determines the activation of GR transcriptional activity.

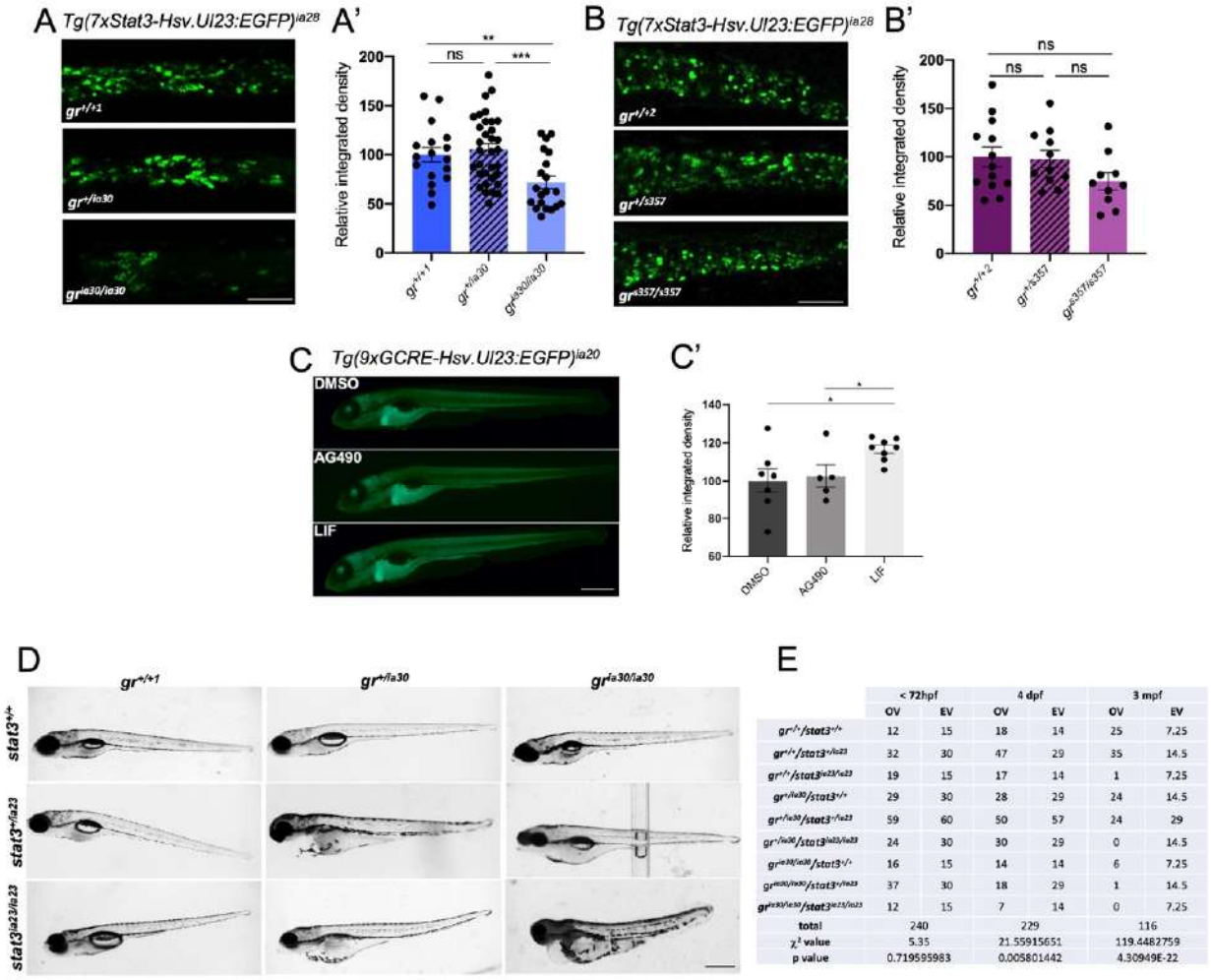

Figure 4. Analysis of crosstalk between GR and Stat3 with zebrafish mutant and transgenic lines. (**A**) Representative pictures (**A'**) and fluorescence quantification (**A'**) of *Tg(7xStat3-Hsv.UI23:EGFP)*^{ia28} 6 dpf larvae at the level of the intestine in $gr^{+/+1}$, $gr^{+/ia30}$ and $gr^{ia30/ia30}$ genetic background. Scale bar= 100 µm. (**B**) Representative pictures (**B**) and fluorescence quantification (**B'**) of *Tg(7xStat3-Hsv.UI23:EGFP)*^{ia28} 6 dpf larvae at the level of the intestine in $gr^{+/+2}$, $gr^{+/s357}$ and $gr^{s357/s357}$ genetic background. Scale bar = 100 µm. (**C**) Representative pictures (**C**) and fluorescence quantification (**C'**) of *Tg(9xGCRE-Hsv.UI23:EGFP)*^{ia20} incubated from 3 to 6 dpf with DMSO, 50 µM AG490 and 20 µM LIF. Scale bar = 500 µm. (**D**) representative pictures of 6 dpf larvae generated by the breeding between $gr^{+/ia30}/stat3^{+/ia23}$ zebrafish. Scale bar = 500 µm. (**E**) Table of observed (OV) and expected (EV) values of animals belonging to the 9 different genotypes obtained from breedings between $gr^{+/ia30}/stat3^{+/ia23}$ zebrafish: χ^2 test shows not significant differences between OV and EV in genotype distribution until 72 hpf (*p*-value = 0.7196); significant differences between OV and EV were detected at 4 dpf (** *p*-value = 0.0058) and 3 mpf (**** *p*-value = 4.30949×10^{-22}). Mean ± SEM. Statistical analyses were performed with Student's *t* test (A,B,C) and χ^2 test (**E**). * $p < 0.05$; ** $p < 0.01$; *** $p < 0.001$; ns = not significant.

Further data showing the different impacts of gr^{ia30} and gr^{s357} mutations on Stat3 are shown in Figure 4D. We bred $gr^{+/ia30}$ mutants with $stat3^{+/ia23}$ larvae and subsequently, we performed $gr^{+/ia30}/stat3^{+/ia23}$ double heterozygotes crosses to obtain the 9 possible genotypes. Interestingly, $gr^{ia30/ia30}/stat3^{ia23/ia23}$ double homozygous mutants are characterized by severe developmental defects like large cardiac oedema, lack of yolk absorption, small head size and start dying at 4 dpf (Figure 4D,E). The severe phenotype of these double mutants was expected, since the roles of Stat3 and GR in development are well-known [53,54]. Interestingly, the defects described above were also detected in $gr^{ia30/ia30}/stat3^{+/ia23}$, $gr^{+/ia30}/stat3^{ia23/ia23}$

and in some of $gr^{+/ia30}/stat3^{+/ia23}$ larvae. Notably, $gr^{ia30/ia30}/stat3^{+/ia23}$ and $gr^{+/ia30}/stat3^{ia23/ia23}$ cannot reach adulthood (Figure 4D,E). Finally, in five breedings between double heterozygous, only three adult $gr^{ia30/ia30}/stat3^{+/ia23}$ have been observed reaching the humane endpoint at 3 months of age. Conversely, the offspring generated by the breeding between $gr^{+/s357}/stat3^{+/ia23}$ double heterozygotes adult zebrafish did not show any morphological defects and adult $gr^{s357/s357}/stat3^{+/ia23}$ have been detected with the expected frequency (12.5%). These results confirmed that GR and Stat3 activities are tightly connected and that GR DNA-binding properties are not required for Stat3 activation and the proper induction of Stat3 transcription.

2.4. GR Regulates Stat3-Transcriptional Activities in DNA-Binding Independent Mechanisms with a Contribution of MR

Further investigations of GR-dependent control of Stat3 transcriptional activity were performed with RT-qPCR analysis of Stat3 target genes in both $gr^{ia30/ia30}$ and $gr^{s357/s357}$ 6 dpf zebrafish larvae. We analysed the levels of expression of *suppressor of cytokine signalling-3a* (*socs3a*), *hypoxia-inducible factor 1α like* (*hif1αl*), *unc-51 like autophagy activating kinase 2* (*ulk2*), *patatin-like phospholipase 3* (*pnpla3*) and *DNA damage-inducible transcript 4* (*ddit4*). *socs3a* is a Stat3 target gene that represses the Jak/Stat3 pathway and binds Janus Kinases (Jaks), inhibiting their function as an activator of Stat3 [55]. The *hif1αl* gene encodes for hypoxia-inducible factor 3α (Hif3α), a factor involved in hypoxia response—a process in which both GR and Stat3 are well-established players [20,56–60]. In addition, its promoter is predicted to harbour Stat3 binding elements (https://maayanlab.cloud/Harmonizome/ accessed on 12 September 2021). Ulk2 is an autophagy inducing kinase and its transcription is positively modulated by Stat3 [61]. *pnpla3* encodes for an enzyme that has hydrolase activity on retinyl esters and triglycerides [62] whereas *ddit4* is upregulated in response to different stressors and its transcription is induced by GCs [63] and phosphorylated Stat3 [64].

socs3a and *hif1αl* expression are not different between $gr^{ia30/ia30}$ and $gr^{s357/s357}$ mutants and their respective WT siblings, meaning that, in basal conditions, they are not differentially expressed in the two genetic backgrounds. Additionally, they are significantly induced in $gr^{+/+}$ upon Dex treatment, confirming their GC-based transcriptional regulation. However, while $gr^{ia30/ia30}$ appeared to be completely insensitive to exogenous GCs (Figure 5A,B), we could observe a not significant increase in *socs3a* and *hif1αl* expression in $gr^{s357/s357}$ larvae upon Dex treatment (Figure 5A′,B′). Evidence about the differential control of Stat3 target gene expression in the two *gr* mutant lines came from the analysis of *ulk2*, *pnpla3* and *ddit4*. Dex significantly induces the expression of these three genes in $gr^{+/+1}$, $gr^{+/+2}$ and $gr^{s357/s357}$, when compared to untreated siblings, but had no effect on $gr^{ia30/ia30}$ larvae (Figure 5A–E,C′–E′). These results demonstrate that GCs regulate the expression of some Stat3-related genes mainly in a GR–DNA binding independent mechanism.

Moreover, we sought to assess whether the differential control of Stat3 target genes observed in $gr^{ia30/ia30}$ and in $gr^{s357/s357}$ can be due to compensating effects by MR. A first analysis of the *mr* mutant in $Tg(7xStat3\text{-}Hsv.Ul23:EGFP)^{ia28}$ Stat3 reporter line background demonstrated that, at least in the intestine, the lack of a functional MR does not affect Stat3-dependent transcription (Figure S2C). However, RT-qPCR analysis of the genes already reported in Figure 4 demonstrated that the absence of a functional MR partially affects the GC-mediated control of Stat3-related genes. As reported in Figure 5, the responsiveness of $mr^{ia32/ia32}$ for Dex is not significantly affected as regards the expression levels of *socs3a*, *hif1αl* and *ddit4*, since we could not see significant differences in their expression in treated $mr^{ia32/ia32}$ compared to treated $mr^{+/+}$. However, *ulk2* and *pnpla3* mRNA expression is not upregulated in mutants, revealing that $mr^{ia32/ia32}$ show defects in the correct expression of Stat3-target genes and demonstrating that MR plays a role in this process together with GR. These transcriptional patterns show that some of these Stat3-dependent genes are controlled by GR alone (like *socs3a*, *hif1αl* and *ddit4*), but other genes, like *pnpla3* and *ulk2*, need both GR and MR to be properly induced. Of note, the basal upregulation of *ddit4*

in $mr^{ia32/ia32}$ compared to $mr^{+/+}$ can be due to the significant upregulation of *nr3c1* that characterizes *mr* KO animals (Figure 2B).

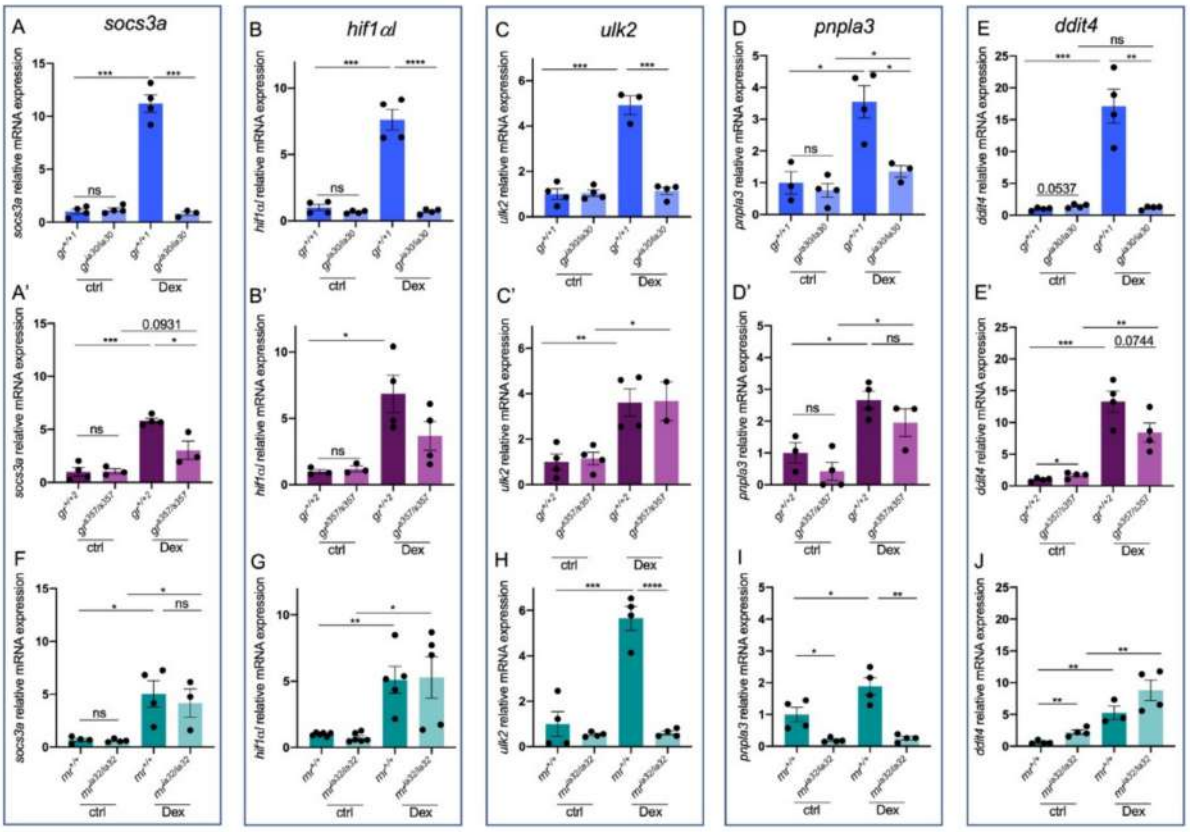

Figure 5. Stat3-dependent genes are differentially expressed in gr^{ia30} and gr^{s357} mutant lines. (**A**) RT-qPCR analysis of *socs3a* in 6 dpf $gr^{+/+}$ and $gr^{ia30/ia30}$ (**A**) and in $gr^{+/+}$ and $gr^{s357/s357}$ (**A′**) larvae with or without Dex treatment. (**B**) RT-qPCR analysis of *hif1αl* in 6 dpf $gr^{+/+}$ and $gr^{ia30/ia30}$ (**B**) and in $gr^{+/+}$ and $gr^{s357/s357}$ (**B′**) larvae with or without Dex treatment. (**C**) RT-qPCR analysis of *ulk2* in 6 dpf $gr^{+/+}$ and $gr^{ia30/ia30}$ (**C**) and in $gr^{+/+}$ and $gr^{s357/s357}$ (**C′**) larvae with or without Dex treatment. (**D**) RT-qPCR analysis of *pnpla3* in 6 dpf $gr^{+/+}$ and $gr^{ia30/ia30}$ (**D**) and in $gr^{+/+}$ and $gr^{s357/s357}$ (**D′**) larvae with or without Dex treatment. (**E**) RT-qPCR analysis of *ddit4* in 6 dpf $gr^{+/+}$ and $gr^{ia30/ia30}$ (**E**) and in $gr^{+/+}$ and $gr^{s357/s357}$ (**E′**) larvae with or without Dex treatment. (**F**) RT-qPCR analysis of *socs3a* in 6 dpf $mr^{+/+}$ and $mr^{ia32/ia32}$ larvae with or without Dex treatment. (**G**) RT-qPCR analysis of *hif1αl* in 6 dpf $mr^{+/+}$ and $mr^{ia32/ia32}$ larvae with or without Dex treatment. (**H**) RT-qPCR analysis of *ddit4* in 6 dpf $mr^{+/+}$ and $mr^{ia32/ia32}$ larvae with or without Dex treatment. (**I**) RT-qPCR analysis of *ulk2* in 6 dpf $mr^{+/+}$ and $mr^{ia32/ia32}$ larvae with or without Dex treatment. (**J**) RT-qPCR analysis of *pnpla3* in 6 dpf $mr^{+/+}$ and $mr^{ia32/ia32}$ larvae with or without Dex treatment. Statistical analyses were performed with Student's *t* test. Mean ± SEM. * $p < 0.05$; ** $p < 0.01$; *** $p < 0.001$; **** $p < 0.0001$; ns = not significant.

3. Discussion

In this work, we decided to investigate the possibility of in vivo distinction between the different GCs-GR mechanisms of transcription regulation. Although the $gr^{s357/s357}$ zebrafish mutant line has been used as a KO model by several research groups [16,20,65–70], our previous works have already suggested that DNA-binding independent mechanisms are still present in the $gr^{s357/s357}$ [14,20]. GR transcriptional activity mechanisms have been debated for a long time. The protein works as a transcription factor in a homodimeric complex binding DNA in several different conformations [71], but some research has also shown that GR monomers can interact with DNA activating the transcription of a small set of target genes [7–9]. Notably, GR activity relies on several phosphorylations that regulate

its interactions with DNA or with other proteins [72] and, recently, GR tetramers have been identified [73,74].

To gain new insights on tethering activity or complex protein–protein–DNA interactions of GR, Escoter-Torres and collaborators [75] generated a mutant mouse line carrying a point mutation in the first zinc finger of the DBD (converting cysteine 437 to glycine). This GR protein cannot bind to DNA, but still maintains the possibility of regulating transcription via protein–protein interactions. Of note, similarly to the GR null mice [5], this model (called $GR^{\Delta Zn}$) is not viable since the embryos die for respiratory failure [75]. Consequently, all studies with both mouse mutant lines need to be performed in vitro, losing the integration of the in vivo models.

Here, with our zebrafish genetic models, we identified functional interactions of zebrafish GR with the MR in the regulation of several GC- and Stat3-related genes and demonstrated that DNA-binding-dependent properties of GR are not essential for inducing the transcription of a portion of GC-dependent genes. Although some canonical GC-responsive genes (such as *klf9*, *epas1a* and *ucp2*) are regulated by GR direct interaction with HREs and do not respond to Dex treatment in both mutants ($gr^{ia30/ia30}$ and $gr^{s357/s357}$), other key GC-related genes have different expression profiles in the two zebrafish lines.

The different features of these mutants helped us to in vivo reveal that GR regulates Stat3 transcriptional activity mainly in a DNA-binding independent way. The expression analysis of some Stat3 targets, *hif1αl*, *ulk2*, *pnpla3* and *ddit4*, showed both that these Stat3 targets are Dex-responsive, and that their responsiveness is independent from GR–DNA-binding: the Dex-related upregulation of these genes was detected in treated $gr^{+/+}$ and $gr^{s357/s357}$ but not in $gr^{ia30/ia30}$, thus confirming a substantial difference between $gr^{ia30/ia30}$ and $gr^{s357/s357}$. We suppose that the GR regulation of Stat3 activity is due to nuclear interactions between these two transcription factors, a tethering mechanism that can control the expression of different target genes without the interaction of GR with HREs [50]. This hypothesis was further confirmed by both the severe phenotype of $gr^{ia30/ia30}/stat3^{ia23/ia23}$ larvae, not detected in $gr^{s357/s357}/stat3^{ia23/ia23}$ mutants, as well as the inability of the $gr^{ia30/ia30}/stat3^{+/ia23}$ and $gr^{+/ia30}/stat3^{ia23/ia23}$ to reach adulthood.

Among the GC-responsive genes we analysed, *ucp2*, a member of the mitochondrial solute carrier 25 family largely involved in mitochondrial homeostasis, also controlled by Stat3 [76,77], is clearly downregulated in $gr^{ia30/ia30}$ compared to $gr^{+/+1}$ siblings. Of note, we could not observe significant differences in *ucp2* expression between $gr^{+/+2}$ and $gr^{s357/s357}$ (Figure 1) suggesting that its basal expression might be regulated by GR in a DNA-binding independent way. However, we did not observe a significant increase of *ucp2* expression after Dex treatment of $gr^{s357/s357}$, implying that *ucp2* regulation by GC depends on the binding of GR to DNA. This trend represents an intermediate expression pattern between the other canonical GC-responsive genes (*klf9* and *epas1a*) and Stat3 canonical targets taken into consideration in our analysis (*hif1αl*, *ulk2*, *pnpla3*, *ddit4*), suggesting that the regulation of GC-related gene expression can be more complex and different between basal and stress conditions (here mimicked with Dex treatment). As observed by Petta et al., and Langlais et al. [49,50] (and recently reviewed by Timmermans and collaborators [78]), the control of transcription factors activities performed by GR can happen in several different conformations and GR participates in this process as a monomer, a dimer or even a tetramer. Notably, STAT3 can be regulated by tethering activities that are lost in $gr^{ia30/ia30}$ mutants but are partially conserved in $gr^{s357/s357}$. Additionally, it has been reported that other steroid hormone receptors, among which is included MR, regulate and are regulated by STAT3 [79–81].

Moreover, we need to keep in mind that GCs can bind GR and MR: two different but related receptors that have a different affinity for corticosteroids. The higher affinity of MR allows the receptor to be occupied in basal conditions while the lower affinity of GR determines its activation in response to GCs-increase following the stress or in phase with the GCs-circadian increase [82].

Both receptors are members of the steroid receptor family and show a high level of similarity: they compete for the same ligands and share the same hormone-responsive elements (HREs) on DNA [21]. Hence, to better understand the mechanisms underlying the differential expression of the genes analysed in basal and GC-stimulated conditions in the *gr* mutant lines, we took into consideration MR and generated a new $mr^{ia32/ia32}$ zebrafish line. The homology between GR and MR and the similar mechanisms of action justify the compensation mechanism detected in both mutant lines: $gr^{ia30/ia30}$ and $mr^{ia32/ia32}$ showed an upregulated expression of respectively *nr3c2* and *nr3c1* transcripts when compared to WT.

Of note, GR and MR can form heterodimers with each other, regulating the expression of specific target genes probably with a different efficacy: more specifically, MR homodimers are the main complex working at low levels of GCs, while MR/GR heterodimers and GR homodimers formations are predominant in stress conditions [21]. This fact can be an interesting starting point for the interpretation of our data. In the $mr^{ia32/ia32}$ line, the expression of canonical GC-dependent genes *klf9* and *epas1a* is downregulated in basal conditions; on the contrary, in $gr^{ia30/ia30}$ *klf9* expression does not show significant differences when compared to $gr^{+/+1}$ and *epas1a* seems to be even more expressed in $gr^{ia30/ia30}$ rather than $gr^{+/+1}$. Interestingly, regarding these two genes, the transcriptional response to Dex is completely erased in both *gr* and *mr* KO lines. Hence, considering the model of Gomez-Sanchez and collaborators [16], we can hypothesize that in basal conditions the expression of *klf9* and *epas1a* is regulated by MR homodimers. For this reason, in $gr^{ia30/ia30}$ line the expression of *klf9* and *epas1a* is not impaired and the upregulation of *nr3c2* in $gr^{ia30/ia30}$ explains the higher levels of expression of *epas1a* in *gr* KO. Upon Dex treatments, the response is possibly driven by GR/MR heterodimers as the sensitivity of these two mutant lines to GCs is severely dampened. Additionally, *pnpla3* also showed expression profiles in mutant lines that are compatible with the mechanism of regulation described by Gomez-Sanchez et al. [21]: GR seems to be not involved in the regulation of their expression in basal conditions, while $mr^{ia32/ia32}$ line showed a downregulated expression of *pnpla3* in basal conditions suggesting that MR homodimers control their transcription. Furthermore, *ulk2* seems to be sensible to Dex stimulation in an MR and GR-dependent way. On the contrary, *hif1αl, ddit4* and *socs3a* do not seem to be regulated by MR: *socs3a* and *hif1αl* levels of expression in basal conditions are not impaired in $mr^{ia32/ia32}$ line, in both basal and stimulated conditions; in the same way, *ddit4* does not show a difference between $mr^{+/+}$ and $mr^{ia32/ia32}$ larvae. Moreover, the significant upregulation in $mr^{ia32/ia32}$ compared to WT suggests the dependency of *ddit4* to GR, since *mr* mutants are characterized by high levels of expression of *gr*. We can conclude that MR probably cooperates with GR in the regulation of some Stat3 targets, regulating both their basal expression (*pnpla3*) and Dex induced response (*pnpla3* and *ulk2*).

Starting from the interesting expression profile of *ucp2* in $gr^{ia30/ia30}$ and $gr^{s357/s357}$ zebrafish lines, we have investigated the expression pattern of other solute carrier family 25 members (*ucp3* and *slc25a25*) to clarify how both MR and GR could be involved in the regulation of mitochondrial homeostasis. These two targets are upregulated by exogenous GCs and their expression relies on GR: in basal conditions the expression of these transcripts is significantly downregulated in *gr* KO compared to WT, but not in $gr^{s357/s357}$ compared to $gr^{+/+2}$, suggesting a basal control of their expression by DNA-binding independent mechanism. After Dex exposure, the scenario slightly changes, and expression profiles demonstrate a more intricate mechanism of regulation. While *ucp2* appears to be regulated by GR-DNA-binding dependent mechanisms, the response to Dex of *ucp3* and *slc25a25* in $gr^{s357/s357}$ is independent from GR-DNA-binding. Interestingly, *ucp2* and *ucp3* genes showed similar expression patterns in $gr^{ia30/ia30}$ and $mr^{ia32/ia32}$, with a downregulation of transcripts in both basal and stimulated conditions compared to $gr^{+/+1}$ and $mr^{+/+}$ respectively, suggesting that both receptors can be involved in the regulation of mitochondrial functions. On the contrary, the basal expression of *slc25a25* in $mr^{ia32/ia32}$ is not impaired, while in $gr^{ia30/ia30}$ it is downregulated. Finally, transcriptional data suggest that both GR

and MR are involved in Dex stimulation of *upc3* and *slc25a25* genes. The level of expression of the analysed genes is summarized in Table 2.

Table 2. Schematic overview of expression of genes analysed in different mutant backgrounds. Non-significant differences are represented with "=", significant downregulation with "⇓" and significant upregulation with "⇑".

Gene	$gr^{ia30/ia30}$ vs. $gr^{+/+1}$		$gr^{s357/s357}$ vs. $gr^{+/+2}$		$mr^{ia32/ia32}$ vs. $mr^{+/+}$	
	ctrl	Dex	ctrl	Dex	ctrl	Dex
klf9	=	⇓	=	⇓	=	⇓
epas1a	⇑	⇓	=	⇓	⇓	⇓
ucp2	⇓	⇓	=	⇓	⇓	⇓
ucp3	⇓	⇓	=	⇑	⇓	⇓
scl25a25a	⇓	⇓	=	⇓	=	⇓
socs3a	=	⇓	=	⇓	=	=
hif1αl	=	⇓	=	=	=	=
ulk2	=	⇓	=	=	=	⇓
pnpla3	=	⇓	=	=	⇓	⇓
ddit4	=	⇓	⇑	=	⇑	⇑

In conclusion, we demonstrated in vivo that GC-dependent genes are regulated through several mechanisms that rely on both GR and MR. As already known, GR exerts its transcriptional activities by both binding directly to HRE, but also by tethering with other transcription factors. Our models allowed us to verify in vivo the two different mechanisms and to demonstrate that Stat3 is one of the most important transcriptional partners of GR. Notably, GR regulates Stat3 transcriptional activity mostly in a DNA-binding independent way, even if we cannot exclude a marginal role of canonical GR transcriptional activities in the modulation of the Jak/Stat3 pathway. Finally, it is worth mentioning that mitochondrial homeostasis is heavily regulated by GR, confirming the strong involvement of this protein in mitochondria activities [83–85]. Notably, the GR effect on the mitochondrial genes here analysed seems to be GR–DNA-binding independent and needs MR to be properly determined. All in all, the results obtained highlight the central role of MR as a prominent regulator and enhancer of GR transcriptional activity and underline the potential of the *gr* KO and $gr^{s357/s357}$ mutants for deepening knowledge on GC-dependent transcriptional mechanisms.

4. Materials and Methods

4.1. Animal Husbandry and Zebrafish Lines

Animals were staged and fed as described by Kimmel et al. [86] and maintained in a large-scale aquaria system. Embryos were obtained after natural mating, raised in Petri dishes containing fish water (50×: 5 g $NaHCO_3$, 39.25 g $CaSO_4$, 25 g Instant Ocean for 1:l) and kept in a 12:12 light/dark cycle at 28 °C. All experimental procedures complied with European Legislation for the Protection of Animals used for Scientific Purposes (Directive 2010/63/EU).

gr^{ia30} [14], mr^{ia32} and $stat3^{ia23}$ [51] mutant lines are genotyped by PCR amplification and 3% agarose gel migration. gr^{s357} animals are genotyped as described in Facchinello et al. [9]. The *Tg(7xStat3-Hsv.Ul23:EGFP)*^{ia28} line and the *Tg(9xGCRE-Hsv.Ul23:EGFP)*^{ia20} line have been respectively characterized by Peron et al. [51] and by Benato et al. [48].

4.2. Generation of mr Zebrafish Mutant Line

The generation of the *mr* mutant zebrafish line was performed using the CRISPR/Cas9-mediated genome editing. Briefly, the CHOPCHOP (https://chopchop.rc.fas.harvard.edu

accessed on 26 January 2022) and E-CRISP (available at http://www.e-crisp.org/E-CRISP/ accessed on 26 January 2022) software were used to design the gene-specific guide RNA (sgRNA) (GAGGCGTCAGGATGCCACTACGG) to target *nr3c2* gene on exon 2 following the protocol described in Gagnon et al. [87]. The guide was subsequently produced using the protocol described in Gagnon et al. [87]. Fertilized eggs were injected with 1 nL of a solution containing 280 ng/µL of Cas9 (M0386T, New England Biolabs) and 3 pmol/µL of *nr3c2*-targeting sgRNA. Genomic DNA was extracted from 4 dpf injected larvae to test the presence of mutations and to confirm the activity of the Cas9 enzyme. Injected embryos were raised to adulthood and screened, by F1 genotyping, for germline transmission of the mutation. An F1 mutant carrier harbouring a deletion of 11 nucleotides was selected and bred with WT to obtain the F2 generation. The resulting heterozygous F2 individuals were incrossed, to obtain F3 generation that includes homozygous mutants.

4.3. Imaging

For in vivo imaging, transgenic larvae were anaesthetized with 0.04% tricaine, embedded in 1% low-melting agarose and mounted on a depression slide. Nikon C2 confocal system was used to acquire images from *Tg(7xStat3-Hsv.Ul23:EGFP)*^{ia28} transgenic larvae. *Tg(9xGCRE-Hsv.Ul23:EGFP)*^{ia20} transgenic larvae were mounted in 1% low-melting agarose and observed with a Leica M165 FC microscope equipped with a Nikon DS-Fi2 digital camera. All images were analysed with Fiji (ImageJ2, Madison, WI, USA) software and fluorescence integrated density was calculated setting a standard threshold on non-fluorescent samples as described in Facchinello et al. [88].

4.4. Animal Treatments

We exposed 6 dpf *gr*$^{+/+}$, *gr*$^{ia30/ia30}$, *gr*$^{s357/s357}$, *mr*$^{+/+}$, and *mr*$^{ia32/ia32}$ larvae to 10 µM Dex for 6 h and the treatments started at 3 p.m. At the end of the treatment, larvae were anaesthetized and sacrificed for RNA extraction. *Tg(9xGCRE-Hsv.Ul23:EGFP)*^{ia20} reporter larvae were treated with 50 µM AG490, 10 µM Dex and 20 µM LIF from 3 to 6 dpf.

4.5. mRNA Isolation and Quantitative Real-Time Reverse Transcription PCR (RT-qPCR)

Total RNAs were extracted from pools of 20 larvae at 6 dpf with TRIzol reagent (Thermo Fisher Scientific, Waltham, MA, USA, 15596018) and incubated at 37 °C for 30 min with RQ1 RNase-Free DNase (Promega, M6101, Madison, WI, USA). cDNA synthesis was performed using random primers (Promega, C1181) and M-MLV Reverse Transcriptase RNase H (Solis BioDyne, 06-21-010000) according to the manufacturer's protocol. qPCRs were performed in triplicate with SybrGreen method by means of CFX384 Touch-Real Time PCR Detection System and the 5x HOT FIREPol EvaGreen qPCR Mix Plus (Solis BioDyne, Tartu, Estonia, 08-36-00001) and *ube2a* and *actb* were used as internal standards in each sample. The amplification protocol consists of 95 °C for 14 min followed by 45 cycles at 95 °C for 20 s, 60 °C for 20 s and 72 °C for 25 s. Threshold cycles (Ct) and melting curves were generated automatically by CFX384 Touch-Real Time PCR Detection System (Biorad, Hercules, CA, USA) and results were obtained with the method described in Livak and Schmittgen [89]. Sequences of genes of interest primers are listed in Table 1.

4.6. Statistical Analysis

Statistical analyses were performed using GraphPad Prism (GraphPad Software Inc., San Diego, CA, USA). Different experimental groups for RT-qPCR and fluorescence quantifications were compared using Student's *t* test. Observed genotype distributions (OV) were compared to the expected values (EV) (+/+ = 25%; +/− = 50%; −/− = 25%) using χ^2 test. * $p < 0.05$; ** $p < 0.01$; *** $p < 0.001$, **** $p < 0.0001$; ns = not significant.

Supplementary Materials: The following are available online at https://www.mdpi.com/article/10.3390/ijms23052678/s1.

Author Contributions: Conceptualization, A.D., L.D.V. and F.A.; methodology, A.D., A.T., C.M.F., D.V., L.B., F.T. and N.F.; validation, A.D., A.T. and C.M.F.; formal analysis, A.D., A.T., P.M., C.R., O.C. and L.D.V.; investigation, A.D., A.T., D.V., L.B., F.T. and N.F.; resources, F.A., O.C. and L.D.V.; writing—original draft preparation, A.D., A.T. and L.D.V.; writing—review and editing, F.A. and L.D.V. All authors have read and agreed to the published version of the manuscript.

Funding: This research was funded by Progetti di Ricerca di Ateneo (CPDA134095), University of Padova (to L.D.V.); Associazione Italiana per la Ricerca sul Cancro grant IG 2017 19928 (to F.A.); Fondo di Ateneo 2019 (to O.C.).

Institutional Review Board Statement: All animal experiments were performed under the permission of the ethical committee of the University of Padova and the Italian Ministero della Salute (23/2015-PR and 112/2015-PR).

Informed Consent Statement: Not applicable.

Data Availability Statement: The data that support the findings of this study are available from the corresponding author upon reasonable request.

Acknowledgments: We are thankful to the personnel at the Zebrafish Centre of the University of Padova (Luigi Pivotti, Shkendy Iljazi, Martina Milanetto and Natascia Tiso). We thank Herwig Baier (Max Planck Institute of Neurobiology, Germany) for sharing the $gr^{s357/s357}$ zebrafish mutant line.

Conflicts of Interest: The authors declare no conflict of interest.

References

1. Binder, E.B. The role of FKBP5, a co-chaperone of the glucocorticoid receptor in the pathogenesis and therapy of affective and anxiety disorders. *Psychoneuroendocrinology* **2009**, *34* (Suppl. 1), S186–S195. [CrossRef]
2. Daneri-Becerra, C.; Zgajnar, N.R.; Lotufo, C.M.; Ramos Hryb, A.B.; Piwien-Pilipuk, G.; Galigniana, M.D. Regulation of FKBP51 and FKBP52 functions by post-translational modifications. *Biochem. Soc. Trans.* **2019**, *47*, 1815–1831. [CrossRef]
3. Helsen, C.; Kerkhofs, S.; Clinckemalie, L.; Spans, L.; Laurent, M.; Boonen, S.; Vanderschueren, D.; Claessens, F. Structural basis for nuclear hormone receptor DNA binding. *Mol. Cell. Endocrinol.* **2012**, *348*, 411–417. [CrossRef]
4. Ratman, D.; Vanden Berghe, W.; Dejager, L.; Libert, C.; Tavernier, J.; Beck, I.M.; De Bosscher, K. How glucocorticoid receptors modulate the activity of other transcription factors: A scope beyond tethering. *Mol. Cell. Endocrinol.* **2013**, *380*, 41–54. [CrossRef]
5. Cole, T.J.; Blendy, J.A.; Monaghan, A.P.; Krieglstein, K.; Schmid, W.; Aguzzi, A.; Fantuzzi, G.; Hummler, E.; Unsicker, K.; Schütz, G. Targeted disruption of the glucocorticoid receptor gene blocks adrenergic chromaffin cell development and severely retards lung maturation. *Genes Dev.* **1995**, *9*, 1608–1621. [CrossRef]
6. Reichardt, H.M.; Tuckermann, J.P.; Bauer, A.; Schütz, G. Molecular genetic dissection of glucocorticoid receptor function in vivo. *Z. Rheumatol.* **2000**, *59* (Suppl. 2), S1–S5. [CrossRef]
7. Liu, W.; Wang, J.; Yu, G.; Pearce, D. Steroid receptor transcriptional synergy is potentiated by disruption of the DNA-binding domain dimer interface. *Mol. Endocrinol.* **1996**, *10*, 1399–1406.
8. Adams, M.; Meijer, O.C.; Wang, J.; Bhargava, A.; Pearce, D. Homodimerization of the glucocorticoid receptor is not essential for response element binding: Activation of the phenylethanolamine *N*-methyltransferase gene by dimerization-defective mutants. *Mol. Endocrinol.* **2003**, *17*, 2583–2592. [CrossRef]
9. Johnson, T.A.; Paakinaho, V.; Kim, S.; Hager, G.L.; Presman, D.M. Genome-wide binding potential and regulatory activity of the glucocorticoid receptor's monomeric and dimeric forms. *Nat. Commun.* **2021**, *12*, 1987. [CrossRef]
10. Gerber, A.N.; Newton, R.; Sasse, S.K. Repression of transcription by the glucocorticoid receptor: A parsimonious model for the genomics era. *J. Biol. Chem.* **2021**, *296*, 100687. [CrossRef]
11. Schiller, B.J.; Chodankar, R.; Watson, L.C.; Stallcup, M.R.; Yamamoto, K.R. Glucocorticoid receptor binds half sites as a monomer and regulates specific target genes. *Genome Biol.* **2014**, *15*, 418. [CrossRef] [PubMed]
12. Dinarello, A.; Licciardello, G.; Fontana, C.M.; Tiso, N.; Argenton, F.; Dalla Valle, L. Glucocorticoid receptor activities in the zebrafish model: A review. *J. Endocrinol.* **2020**, *247*, R63–R82. [CrossRef]
13. Schaaf, M.J.; Chatzopoulou, A.; Spaink, H.P. The zebrafish as a model system for glucocorticoid receptor research. *Comp. Biochem. Physiol. A Mol. Integr. Physiol.* **2009**, *153*, 75–82. [CrossRef]
14. Facchinello, N.; Skobo, T.; Meneghetti, G.; Colletti, E.; Dinarello, A.; Tiso, N.; Costa, R.; Gioacchini, G.; Carnevali, O.; Argenton, F.; et al. nr3c1 null mutant zebrafish are viable and reveal DNA-binding-independent activities of the glucocorticoid receptor. *Sci. Rep.* **2017**, *7*, 4371. [CrossRef]
15. Muto, A.; Orger, M.B.; Wehman, A.M.; Smear, M.C.; Kay, J.N.; Page-McCaw, P.S.; Gahtan, E.; Xiao, T.; Nevin, L.M.; Gosse, N.J.; et al. Forward genetic analysis of visual behavior in zebrafish. *PLoS Genet.* **2005**, *1*, e66. [CrossRef]
16. Ziv, L.; Muto, A.; Schoonheim, P.J.; Meijsing, S.H.; Strasser, D.; Ingraham, H.A.; Schaaf, M.J.; Yamamoto, K.R.; Baier, H. An affective disorder in zebrafish with mutation of the glucocorticoid receptor. *Mol. Psychiatry* **2013**, *18*, 681–691. [CrossRef]

17. Morbiato, E.; Frigato, E.; Dinarello, A.; Maradonna, F.; Facchinello, N.; Argenton, F.; Carnevali, O.; Dalla Valle, L.; Bertolucci, C. Feeding Entrainment of the Zebrafish Circadian Clock Is Regulated by the Glucocorticoid Receptor. *Cells* **2019**, *8*, 1342. [CrossRef]
18. Maradonna, F.; Gioacchini, G.; Notarstefano, V.; Fontana, C.M.; Citton, F.; Dalla Valle, L.; Giorgini, E.; Carnevali, O. Knockout of the Glucocorticoid Receptor Impairs Reproduction in Female Zebrafish. *Int. J. Mol. Sci.* **2020**, *21*, 9073. [CrossRef]
19. Griffiths, B.B.; Schoonheim, P.J.; Ziv, L.; Voelker, L.; Baier, H.; Gahtan, E. A zebrafish model of glucocorticoid resistance shows serotonergic modulation of the stress response. *Front. Behav. Neurosci.* **2012**, *6*, 68. [CrossRef]
20. Vettori, A.; Greenald, D.; Wilson, G.K.; Peron, M.; Facchinello, N.; Markham, E.; Sinnakaruppan, M.; Matthews, L.C.; McKeating, J.A.; Argenton, F.; et al. Glucocorticoids promote Von Hippel Lindau degradation and Hif-1α stabilization. *Proc. Natl. Acad. Sci. USA* **2017**, *114*, 9948–9953. [CrossRef]
21. Gomez-Sanchez, E.; Gomez-Sanchez, C.E. The multifaceted mineralocorticoid receptor. *Comp. Physiol.* **2014**, *4*, 965–994.
22. Rivers, C.A.; Rogers, M.F.; Stubbs, F.E.; Conway-Campbell, B.L.; Lightman, S.L.; Pooley, J.R. Glucocorticoid Receptor-Tethered Mineralocorticoid Receptors Increase Glucocorticoid-Induced Transcriptional Responses. *Endocrinology* **2019**, *160*, 1044–1056. [CrossRef]
23. Savory, J.G.; Préfontaine, G.G.; Lamprecht, C.; Liao, M.; Walther, R.F.; Lefebvre, Y.A.; Haché, R.J. Glucocorticoid receptor homodimers and glucocorticoid-mineralocorticoid receptor heterodimers form in the cytoplasm through alternative dimerization interfaces. *Mol. Cell. Biol.* **2001**, *21*, 781–793. [CrossRef]
24. Pooley, J.R.; Rivers, C.A.; Kilcooley, M.T.; Paul, S.N.; Cavga, A.D.; Kershaw, Y.M.; Muratcioglu, S.; Gursoy, A.; Keskin, O.; Lightman, S.L. Beyond the heterodimer model for mineralocorticoid and glucocorticoid receptor interactions in nuclei and at DNA. *PLoS ONE* **2020**, *15*, e0227520. [CrossRef]
25. Mifsud, K.R.; Reul, J.M. Acute stress enhances heterodimerization and binding of corticosteroid receptors at glucocorticoid target genes in the hippocampus. *Proc. Natl. Acad. Sci. USA* **2016**, *113*, 11336–11341. [CrossRef]
26. Kellendonk, C.; Gass, P.; Kretz, O.; Schütz, G.; Tronche, F. Corticosteroid receptors in the brain: Gene targeting studies. *Brain Res. Bull.* **2002**, *57*, 73–83. [CrossRef]
27. Harris, A.P.; Holmes, M.C.; de Kloet, E.R.; Chapman, K.E.; Seckl, J.R. Mineralocorticoid and glucocorticoid receptor balance in control of HPA axis and behaviour. *Psychoneuroendocrinology* **2013**, *38*, 648–658. [CrossRef]
28. De Kloet, E.R. Hormones and the stressed brain. *Ann. N. Y. Acad. Sci.* **2004**, *1018*, 1–15. [CrossRef]
29. DeRijk, R.H.; de Kloet, E.R.; Zitman, F.G.; van Leeuwen, N. Mineralocorticoid receptor gene variants as determinants of HPA axis regulation and behavior. *Endocr. Dev.* **2011**, *20*, 137–148.
30. Qi, X.R.; Kamphuis, W.; Wang, S.; Wang, Q.; Lucassen, P.J.; Zhou, J.N.; Swaab, D.F. Aberrant stress hormone receptor balance in the human prefrontal cortex and hypothalamic paraventricular nucleus of depressed patients. *Psychoneuroendocrinology* **2013**, *38*, 863–870. [CrossRef]
31. Takahashi, H.; Sakamoto, T. The role of 'mineralocorticoids' in teleost fish: Relative importance of glucocorticoid signaling in the osmoregulation and 'central' actions of mineralocorticoid receptor. *Gen. Comp. Endocrinol.* **2013**, *181*, 223–228. [CrossRef]
32. Faught, E.; Vijayan, M.M. The mineralocorticoid receptor is essential for stress axis regulation in zebrafish larvae. *Sci. Rep.* **2018**, *8*, 18081. [CrossRef]
33. Hu, X.; Funder, J.W. The evolution of mineralocorticoid receptors. *Mol. Endocrinol.* **2006**, *20*, 1471–1478. [CrossRef]
34. Funder, J.W. Mineralocorticoid receptors: Distribution and activation. *Heart Fail. Rev.* **2005**, *10*, 15–22. [CrossRef]
35. Lin, C.H.; Tsai, I.L.; Su, C.H.; Tseng, D.Y.; Hwang, P.P. Reverse effect of mammalian hypocalcemic cortisol in fish: Cortisol stimulates Ca2+ uptake via glucocorticoid receptor-mediated vitamin D3 metabolism. *PLoS ONE* **2011**, *6*, e23689. [CrossRef]
36. Kumai, Y.; Nesan, D.; Vijayan, M.M.; Perry, S.F. Cortisol regulates Na+ uptake in zebrafish, *Danio rerio*, larvae via the glucocorticoid receptor. *Mol. Cell. Endocrinol.* **2012**, *364*, 113–125. [CrossRef]
37. Cruz, S.A.; Lin, C.H.; Chao, P.L.; Hwang, P.P. Glucocorticoid receptor, but not mineralocorticoid receptor, mediates cortisol regulation of epidermal ionocyte development and ion transport in zebrafish (*Danio rerio*). *PLoS ONE* **2013**, *8*, e77997. [CrossRef]
38. Kwong, R.W.; Perry, S.F. Cortisol regulates epithelial permeability and sodium losses in zebrafish exposed to acidic water. *J. Endocrinol.* **2013**, *217*, 253–264. [CrossRef]
39. Lin, C.H.; Shih, T.H.; Liu, S.T.; Hsu, H.H.; Hwang, P.P. Cortisol Regulates Acid Secretion of H(+)-ATPase-rich Ionocytes in Zebrafish (*Danio rerio*) Embryos. *Front. Physiol.* **2015**, *6*, 328. [CrossRef] [PubMed]
40. Lin, C.H.; Hu, H.J.; Hwang, P.P. Cortisol regulates sodium homeostasis by stimulating the transcription of sodium-chloride transporter (NCC) in zebrafish (*Danio rerio*). *Mol. Cell. Endocrinol.* **2016**, *422*, 93–102. [CrossRef]
41. Kuo, T.; Liu, P.H.; Chen, T.C.; Lee, R.A.; New, J.; Zhang, D.; Lei, C.; Chau, A.; Tang, Y.; Cheung, E.; et al. Transcriptional regulation of FoxO3 gene by glucocorticoids in murine myotubes. *Am. J. Physiol. Endocrinol. Metab.* **2016**, *310*, E572–E585. [CrossRef]
42. Gans, I.; Hartig, E.I.; Zhu, S.; Tilden, A.R.; Hutchins, L.N.; Maki, N.J.; Graber, J.H.; Coffman, J.A. Klf9 is a key feedforward regulator of the transcriptomic response to glucocorticoid receptor activity. *Sci. Rep.* **2020**, *10*, 11415. [CrossRef]
43. Ijichi, N.; Ikeda, K.; Fujita, M.; Usui, T.; Urano, T.; Azuma, K.; Ouchi, Y.; Horie-Inoue, K.; Inue, S. EPAS1, a dexamethasone-inducible gene in osteoblasts, inhibits osteoblastic differentiation. *Open Bone J.* **2009**, *1*, 28–37. [CrossRef]
44. Rog-Zielinska, E.A.; Craig, M.A.; Manning, J.R.; Richardson, R.V.; Gowans, G.J.; Dunbar, D.R.; Gharbi, K.; Kenyon, C.J.; Holmes, M.C.; Hardie, D.G.; et al. Glucocorticoids promote structural and functional maturation of foetal cardiomyocytes: A role for PGC-1α. *Cell Death Differ.* **2015**, *22*, 1106–1116. [CrossRef]

45. Brand, M.D.; Esteves, T.C. Physiological functions of the mitochondrial uncoupling proteins UCP2 and UCP3. *Cell Metab.* **2005**, *2*, 85–93. [CrossRef]
46. Weber, K.; Brück, P.; Mikes, Z.; Küpper, J.H.; Klingenspor, M.; Wiesner, R.J. Glucocorticoid hormone stimulates mitochondrial biogenesis specifically in skeletal muscle. *Endocrinology* **2002**, *143*, 177–184. [CrossRef]
47. Ma, Z.; Chen, J. Premature Termination Codon-Bearing mRNA Mediates Genetic Compensation Response. *Zebrafish* **2020**, *17*, 157–162. [CrossRef]
48. Benato, F.; Colletti, E.; Skobo, T.; Moro, E.; Colombo, L.; Argenton, F.; Dalla Valle, L. A living biosensor model to dynamically trace glucocorticoid transcriptional activity during development and adult life in zebrafish. *Mol. Cell. Endocrinol.* **2014**, *392*, 60–72. [CrossRef]
49. Petta, I.; Dejager, L.; Ballegeer, M.; Lievens, S.; Tavernier, J.; De Bosscher, K.; Libert, C. The Interactome of the Glucocorticoid Receptor and Its Influence on the Actions of Glucocorticoids in Combatting Inflammatory and Infectious Diseases. *Microbiol. Mol. Biol. Rev.* **2016**, *80*, 495–522. [CrossRef]
50. Langlais, D.; Couture, C.; Balsalobre, A.; Drouin, J. The Stat3/GR interaction code: Predictive value of direct/indirect DNA recruitment for transcription outcome. *Mol. Cell* **2012**, *47*, 38–49. [CrossRef]
51. Peron, M.; Dinarello, A.; Meneghetti, G.; Martorano, L.; Facchinello, N.; Vettori, A.; Licciardello, G.; Tiso, N.; Argenton, F. The stem-like Stat3-responsive cells of zebrafish intestine are Wnt/β-catenin dependent. *Development* **2020**, *147*, dev188987. [CrossRef]
52. Peron, M.; Dinarello, A.; Meneghetti, G.; Martorano, L.; Betto, R.M.; Facchinello, N.; Tesoriere, A.; Tiso, N.; Martello, G.; Argenton, F. Y705 and S727 are required for the mitochondrial import and transcriptional activities of STAT3, and for regulation of stem cell proliferation. *Development* **2021**, *148*, dev199477. [CrossRef]
53. Yamashita, S.; Miyagi, C.; Carmany-Rampey, A.; Shimizu, T.; Fujii, R.; Schier, A.F.; Hirano, T. Stat3 Controls Cell Movements during Zebrafish Gastrulation. *Dev Cell* **2002**, *2*, 363–375. [CrossRef]
54. Pikulkaew, S.; Benato, F.; Celeghin, A.; Zucal, C.; Skobo, T.; Colombo, L.; Dalla Valle, L. The knockdown of maternal glucocorticoid receptor mRNA alters embryo development in zebrafish. *Dev. Dyn.* **2011**, *240*, 874–889. [CrossRef]
55. Carow, B.; Rottenberg, M.E. SOCS3, a Major Regulator of Infection and Inflammation. *Front. Immunol.* **2014**, *5*, 58. [CrossRef]
56. Jung, J.E.; Lee, H.G.; Cho, I.H.; Chung, D.H.; Yoon, S.H.; Yang, Y.M.; Lee, J.W.; Choi, S.; Park, J.W.; Ye, S.K.; et al. STAT3 is a potential modulator of HIF-1-mediated VEGF expression in human renal carcinoma cells. *FASEB J.* **2005**, *19*, 1296–1298. [CrossRef]
57. Xu, Q.; Briggs, J.; Park, S.; Niu, G.; Kortylewski, M.; Zhang, S.; Gritsko, T.; Turkson, J.; Kay, H.; Semenza, G.L.; et al. Targeting Stat3 blocks both HIF-1 and VEGF expression induced by multiple oncogenic growth signaling pathways. *Oncogene* **2005**, *24*, 5552–5560. [CrossRef]
58. Cui, Y.; Li, Y.Y.; Li, J.; Zhang, H.Y.; Wang, F.; Bai, X.; Li, S.S. STAT3 regulates hypoxia-induced epithelial mesenchymal transition in oesophageal squamous cell cancer. *Oncol. Rep.* **2016**, *36*, 108–116. [CrossRef]
59. Marchi, D.; Santhakumar, K.; Markham, E.; Li, N.; Storbeck, K.H.; Krone, N.; Cunliffe, V.T.; van Eeden, F.J.M. Bidirectional crosstalk between Hypoxia-Inducible Factor and glucocorticoid signalling in zebrafish larvae. *PLoS Genet.* **2020**, *16*, e1008757. [CrossRef]
60. Dinarello, A.; Betto, R.M.; Cioccarelli, C.; Diamante, L.; Meneghetti, G.; Peron, M.; Tesoriere, A.; Laquatra, C.; Tiso, N.; Martello, G.; et al. STAT3 and HIF1α cooperatively mediate the transcriptional and physiological responses to hypoxia. *bioRxiv* **2021**. [CrossRef]
61. You, L.; Wang, Z.; Li, H.; Shou, J.; Jing, Z.; Xie, J.; Sui, X.; Pan, H.; Han, W. The role of STAT3 in autophagy. *Autophagy* **2015**, *11*, 729–739. [CrossRef]
62. Dong, X.C. PNPLA3-A Potential Therapeutic Target for Personalized Treatment of Chronic Liver Disease. *Front. Med.* **2019**, *6*, 304. [CrossRef]
63. Tirado-Hurtado, I.; Fajardo, W.; Pinto, J.A. DNA Damage Inducible Transcript 4 Gene: The Switch of the Metabolism as Potential Target in Cancer. *Front. Oncol.* **2018**, *8*, 106. [CrossRef]
64. Li, T.; Zhang, G.; Wang, L.; Li, S.; Xu, X.; Gao, Y. Defects in mTORC1 Network and mTORC1-STAT3 Pathway Crosstalk Contributes to Non-inflammatory Hepatocellular Carcinoma. *Front. Cell Dev. Biol.* **2020**, *8*, 225. [CrossRef]
65. Muto, A.; Taylor, M.R.; Suzawa, M.; Korenbrot, J.I.; Baier, H. Glucocorticoid receptor activity regulates light adaptation in the zebrafish retina. *Front. Neural Circuits* **2013**, *7*, 145. [CrossRef]
66. Chatzopoulou, A.; Heijmans, J.P.; Burgerhout, E.; Oskam, N.; Spaink, H.P.; Meijer, A.H.; Schaaf, M.J. Glucocorticoid-Induced Attenuation of the Inflammatory Response in Zebrafish. *Endocrinology* **2016**, *157*, 2772–2784. [CrossRef]
67. Kwan, W.; Cortes, M.; Frost, I.; Esain, V.; Theodore, L.N.; Liu, S.Y.; Budrow, N.; Goessling, W.; North, T.E. The Central Nervous System Regulates Embryonic HSPC Production via Stress-Responsive Glucocorticoid Receptor Signaling. *Cell Stem Cell* **2016**, *19*, 370–382. [CrossRef]
68. Spulber, S.; Raciti, M.; Dulko-Smith, B.; Lupu, D.; Rüegg, J.; Nam, K.; Ceccatelli, S. Methylmercury interferes with glucocorticoid receptor: Potential role in the mediation of developmental neurotoxicity. *Toxicol. Appl. Pharmacol.* **2018**, *354*, 94–100. [CrossRef]
69. Hayward, T.; Young, A.; Jiang, A.; Crespi, E.J.; Coffin, A.B. Glucococorticoid receptor activation exacerbates aminoglycoside-induced damage to the zebrafish lateral line. *Hear. Res.* **2019**, *377*, 12–23. [CrossRef]
70. Brun, N.R.; van Hage, P.; Hunting, E.R.; Haramis, A.G.; Vink, S.C.; Vijver, M.G.; Schaaf, M.J.M.; Tudorache, C. Polystyrene nanoplastics disrupt glucose metabolism and cortisol levels with a possible link to behavioural changes in larval zebrafish. *Commun. Biol.* **2019**, *2*, 382. [CrossRef]

71. Vettorazzi, S.; Nalbantoglu, D.; Gebhardt, J.C.M.; Tuckermann, J. A guide to changing paradigms of glucocorticoid receptor function-a model system for genome regulation and physiology. *FEBS J.* **2021**, *2*, febs.16100. [CrossRef]
72. Escoter-Torres, L.; Caratti, G.; Mechtidou, A.; Tuckermann, J.; Uhlenhaut, N.H.; Vettorazzi, S. Fighting the Fire: Mechanisms of Inflammatory Gene Regulation by the Glucocorticoid Receptor. *Front Immunol.* **2019**, *10*, 1859. [CrossRef] [PubMed]
73. Payvar, F.; DeFranco, D.; Firestone, G.L.; Edgar, B.; Wrange, O.; Okret, S.; Gustafsson, J.A.; Yamamoto, K.R. Sequence-specific binding of glucocorticoid receptor to MTV DNA at sites within and upstream of the transcribed region. *Cell* **1983**, *35 Pt 1*, 381–392. [CrossRef]
74. Presman, D.M.; Ganguly, S.; Schiltz, R.L.; Johnson, T.A.; Karpova, T.S.; Hager, G.L. DNA binding triggers tetramerization of the glucocorticoid receptor in live cells. *Proc. Natl. Acad. Sci. USA* **2016**, *113*, 8236–8241. [CrossRef] [PubMed]
75. Escoter-Torres, L.; Greulich, F.; Quagliarini, F.; Wierer, M.; Uhlenhaut, N.H. Anti-inflammatory functions of the glucocorticoid receptor require DNA binding. *Nucleic Acids Res.* **2020**, *48*, 8393–8407. [CrossRef]
76. Gerö, D.; Szabo, C. Glucocorticoids Suppress Mitochondrial Oxidant Production via Upregulation of Uncoupling Protein 2 in Hyperglycemic Endothelial Cells. *PLoS ONE* **2016**, *11*, e0154813. [CrossRef]
77. Lapp, D.W.; Zhang, S.S.; Barnstable, C.J. Stat3 mediates LIF-induced protection of astrocytes against toxic ROS by upregulating the UPC2 mRNA pool. *Glia* **2014**, *62*, 159–170. [CrossRef]
78. Timmermans, S.; Souffriau, J.; Libert, C. A General Introduction to Glucocorticoid Biology. *Front. Immunol.* **2019**, *10*, 1545. [CrossRef]
79. Zheng, X.J.; Liu, Y.; Zhang, W.C.; Liu, Y.; Li, C.; Sun, X.N.; Zhang, Y.Y.; Xu, J.; Jiang, X.; Zhang, L.; et al. Mineralocorticoid receptor negatively regulates angiogenesis through repression of STAT3 activity in endothelial cells. *J. Pathol.* **2019**, *248*, 438–451. [CrossRef]
80. De Miguel, F.; Lee, S.O.; Onate, S.A.; Gao, A.C. Stat3 enhances transactivation of steroid hormone receptors. *Nucl. Recept.* **2003**, *1*, 3. [CrossRef]
81. Queisser, N.; Schupp, N.; Schwarz, E.; Hartmann, C.; Mackenzie, G.G.; Oteiza, P.I. Aldosterone activates the oncogenic signals ERK1/2 and STAT3 via redox-regulated mechanisms. *Mol. Carcinog.* **2017**, *56*, 1868–1883. [CrossRef]
82. De Kloet, E.R.; Joëls, M.; Holsboer, F. Stress and the brain: From adaptation to disease. *Nat. Rev. Neurosci.* **2005**, *6*, 463–475. [CrossRef]
83. Psarra, A.M.; Sekeris, C.E. Glucocorticoids induce mitochondrial gene transcription in HepG2 cells: Role of the mitochondrial glucocorticoid receptor. *Biochim. Biophys. Acta* **2011**, *1813*, 1814–1821. [CrossRef]
84. Lapp, H.E.; Bartlett, A.A.; Hunter, R.G. Stress and glucocorticoid receptor regulation of mitochondrial gene expression. *J. Mol. Endocrinol.* **2019**, *62*, R121–R128. [CrossRef]
85. Kokkinopoulou, I.; Moutsatsou, P. Mitochondrial Glucocorticoid Receptors and Their Actions. *Int. J. Mol. Sci.* **2021**, *22*, 6054. [CrossRef]
86. Kimmel, C.B.; Ballard, W.W.; Kimmel, S.R.; Ullmann, B.; Schilling, T.F. Stages of embryonic development of the zebrafish. *Dev. Dyn.* **1995**, *203*, 253–310. [CrossRef]
87. Gagnon, J.A.; Valen, E.; Thyme, S.B.; Huang, P.; Akhmetova, L.; Pauli, A.; Montague, T.G.; Zimmerman, S.; Richter, C.; Schier, A.F. Efficient mutagenesis by Cas9 protein-mediated oligonucleotide insertion and large-scale assessment of single-guide RNAs. *PLoS ONE* **2014**, *9*, e98186. [CrossRef]
88. Facchinello, N.; Schiavone, M.; Vettori, A.; Argenton, F.; Tiso, N. Monitoring Wnt Signaling in Zebrafish Using Fluorescent Biosensors. *Methods Mol. Biol.* **2016**, *1481*, 81–94.
89. Livak, K.J.; Schmittgen, T.D. Analysis of relative gene expression data using real-time quantitative PCR and the $2^{-\Delta\Delta C_T}$ Method. *Methods* **2001**, *25*, 402–408. [CrossRef]